

Keywords: Riluzole; SKA-31; E4031; Cisplatin uptake; preclinical mouse models

The combined activation of $K_{Ca}3.1$ and inhibition of $K_v11.1$ /hERG1 currents contribute to overcome Cisplatin resistance in colorectal cancer cells

Serena Pillozzi^{1,9}, Massimo D'Amico^{2,9}, Gianluca Bartoli¹, Luca Gasparoli¹, Giulia Petroni¹, Olivia Crociani¹, Tiziano Marzo^{3,4}, Angela Guerriero¹, Luigi Messori³, Mirko Severi⁵, Roberto Udisti⁵, Heike Wulff⁶, K George Chandy⁷, Andrea Becchetti⁸ and Annarosa Arcangeli^{*1}

¹Department of Experimental and Clinical Medicine, Section of Internal Medicine, University of Florence, Viale G.B. Morgagni 50, 50134 Firenze, Italy; ²DIVAL Toscana Srl, Via Madonna del Piano 6, Sesto Fiorentino, 50119 Firenze, Italy; ³Laboratory of Metals in Medicine (MetMed), Department of Chemistry, University of Florence, Via della Lastruccia 3, Sesto Fiorentino, 50019 Florence, Italy; ⁴Department of Chemistry and Industrial Chemistry (DCCI), University of Pisa, Via Moruzzi 13, 56124 Pisa, Italy; ⁵Department of Chemistry, University of Florence, Via della Lastruccia 3, Sesto Fiorentino, 50019 Florence, Italy; ⁶Department of Pharmacology, 451 Health Sciences Drive, University of California, Davis, CA 95616, USA; ⁷Laboratory of Molecular Physiology in the Infection and Immunity Theme, Lee Kong Chian School of Medicine, Nanyang Technological University, 50 Nanyang Avenue, Singapore 639798, Singapore and ⁸Department of Biotechnology and Biosciences, University of Milano-Bicocca, Piazza della Scienza 2, 20126 Milano, Italy

Background: Platinum-based drugs such as Cisplatin are commonly employed for cancer treatment. Despite an initial therapeutic response, Cisplatin treatment often results in the development of chemoresistance. To identify novel approaches to overcome Cisplatin resistance, we tested Cisplatin in combination with K^+ channel modulators on colorectal cancer (CRC) cells.

Methods: The functional expression of Ca^{2+} -activated ($K_{Ca}3.1$, also known as KCNN4) and voltage-dependent ($K_v11.1$, also known as KCNH2 or hERG1) K^+ channels was determined in two CRC cell lines (HCT-116 and HCT-8) by molecular and electrophysiological techniques. Cisplatin and several K^+ channel modulators were tested *in vitro* for their action on K^+ currents, cell vitality, apoptosis, cell cycle, proliferation, intracellular signalling and Platinum uptake. These effects were also analysed in a mouse model mimicking Cisplatin resistance.

Results: Cisplatin-resistant CRC cells expressed higher levels of $K_{Ca}3.1$ and $K_v11.1$ channels, compared with Cisplatin-sensitive CRC cells. In resistant cells, $K_{Ca}3.1$ activators (SKA-31) and $K_v11.1$ inhibitors (E4031) had a synergistic action with Cisplatin in triggering apoptosis and inhibiting proliferation. The effect was maximal when $K_{Ca}3.1$ activation and $K_v11.1$ inhibition were combined. In fact, similar results were produced by Riluzole, which is able to both activate $K_{Ca}3.1$ and inhibit $K_v11.1$. Cisplatin uptake into resistant cells depended on $K_{Ca}3.1$ channel activity, as it was potentiated by $K_{Ca}3.1$ activators. $K_v11.1$ blockade led to increased $K_{Ca}3.1$ expression and thereby stimulated Cisplatin uptake. Finally, the combined administration of a $K_{Ca}3.1$ activator and a $K_v11.1$ inhibitor also overcame Cisplatin resistance *in vivo*.

Conclusions: As Riluzole, an activator of $K_{Ca}3.1$ and inhibitor of $K_v11.1$ channels, is in clinical use, our results suggest that this compound may be useful in the clinic to improve Cisplatin efficacy and overcome Cisplatin resistance in CRC.

*Correspondence: Professor A Arcangeli, E-mail: annarosa.arcangeli@unifi.it

⁹These authors contributed equally to this work.

Received 29 July 2017; revised 25 September 2017; accepted 2 October 2017; published online 21 November 2017

© 2018 Cancer Research UK. All rights reserved 0007–0920/18

Platinum-based drugs and, in particular, *cis*-diamminedichlorido-platinum (II), best known as Cisplatin, are employed for the treatment of a wide range of solid malignancies, including colorectal cancer (CRC). Cisplatin exerts anticancer effects by inducing the formation of platinum–DNA adducts (Huang *et al*, 1995), which in turn trigger the apoptotic process (Wang and Lippard, 2005). Cisplatin also produces ‘non-genomic effects’, affecting plasma membrane proteins, including ion channels and transporters, and cytoskeletal components. Such effects are often related to Cisplatin side effects, such as peripheral neuropathy (Carozzi *et al*, 2015).

Despite a consistent rate of initial responses, Cisplatin treatment often results in the development of resistance, leading to therapeutic failure. Intense research has identified several mechanisms underlying Cisplatin resistance (Galluzzi *et al*, 2014). Among them, reduced uptake of Cisplatin through the plasma membrane is one of the most critical ‘pretarget’ steps of resistance development. Cisplatin is taken up by both simple and facilitated diffusion (Yoshida *et al*, 1994; Ishida *et al*, 2002). Relevant in the latter process are the copper (Cu) transporters CTR1 and CTR2, encoded by the *SLC31A* genes 1 and 2, respectively. Altered levels or mis-functionality of CTR1 and CTR2 are consistently associated with Cisplatin resistance (Katano *et al*, 2002; Huang *et al*, 2014). Moreover, extrusion of the drug by two P-type ATPases, ATP7A and ATP7B is also operant. Altered expression and cellular localisation of such ATPases has been linked to the occurrence of Cisplatin resistance in ovarian cancer (Kalayda *et al*, 2008). Plasma membrane transporters are not only involved in the transport of the drug but can also be affected by Cisplatin itself (Shimizu *et al*, 2008). For example, when apoptosis is triggered, an early persistent shrinkage (named apoptotic volume decrease) results as a consequence of efflux of K⁺ and the activation of an outwardly rectifying Cl[−] current. The latter has the electrophysiological and pharmacological characteristics of volume regulated anion channels (VRAC) (Lang and Hoffmann, 2012). Recently, VRAC, and in particular the LRCC8A and LRCC8D molecular components, have been shown to influence Cisplatin uptake (Jentsch *et al*, 2016). Not surprisingly, a reduction of anion currents through VRAC has been linked to Cisplatin chemoresistance (Lee *et al*, 2008; Poulsen *et al*, 2010).

K⁺ channels are frequently dysregulated in cancer (Arcangeli *et al*, 2009; D’Amico *et al*, 2013). In particular, K_{Ca}3.1 and K_v11.1 are upregulated during tumour progression (Lastraioli *et al*, 2004; Muratori *et al*, 2016) and contribute to malignancy, which includes chemoresistance (Pillozzi *et al*, 2011). Interestingly, Cisplatin sensitivity is related to K⁺ channel expression and activity in several cancer cell lines (Lee *et al*, 2008; Zhang *et al*, 2012; Leanza *et al*, 2014; Hui *et al*, 2015; Samuel *et al*, 2016). For example, increased activity of intermediate-conductance K_{Ca}3.1 (KCNN4) calcium-activated K⁺ currents (*I*_{IK}) contributes to Cisplatin sensitivity in epidermoid cancer cells (Lee *et al*, 2008) and *I*_{IK} activation consistently potentiates Cisplatin-induced cytotoxicity. In contrast, expression of large-conductance K_{Ca}1.1 (KCNMA1, BK) calcium-activated channels is reduced in Cisplatin-resistant ovarian cells (Samuel *et al*, 2016). In patients with ovarian cancer treated with Cisplatin-based adjuvant chemotherapy, decreased expression of K_v10.1 (KCNH1, Eag1) correlates with favourable prognosis and predicts Cisplatin sensitivity in ovarian cancer cells (Hui *et al*, 2015). K_v11.1 (hERG1) channels have been found to be upregulated by Cisplatin in gastric cancer cells, and their silencing decreases the cytotoxic effects of the drug (Zhang *et al*, 2012). Moreover, a clear correlation between K⁺ channel expression and Cisplatin sensitivity was shown in cancer cell lines of different histogenesis (Leanza *et al*, 2014).

Here we investigated the role of K⁺ channels in Cisplatin resistance in CRC and tested the possibility of overcoming Cisplatin resistance with K⁺ channel-modulating agents.

MATERIALS AND METHODS

Chemicals and antibodies. Unless otherwise indicated, all chemicals, drugs and antibodies were from Sigma-Aldrich, Milan, Italy. For *in vitro* experiments Riluzole, SKA-31 and TRAM-34 were dissolved in DMSO, at a concentration of 5 mM, whereas for *in vivo* experiments Riluzole was dissolved in 5% Kolliphor in 0.9% NaCl. E4031 dihydrochloride, Cisplatin and Oxaliplatin were dissolved in bi-distilled water. All stock solutions were stored at -20 °C. The list of antibodies and the concentrations used for western blotting (WB) experiments are reported in Supplementary Methods.

Cell culture. All the CRC cell lines were cultured in RPMI-1640 medium (Euroclone; Milan, Italy), supplemented with 2% L-Glut, 10% foetal bovine serum (Euroclone) and 1% penicillin/streptomycin (complete medium). HCT-116 cells were obtained from the American Type Culture Collection ATCC (Manassas, VA, USA); HT-29 cells were kindly provided by Dr R Falcioni (Regina Elena Cancer Institute, Roma, Italy); HCT-8 and H630 were kindly provided by Dr E Mini (University of Florence, Florence, Italy).

Total RNA extraction, reverse transcription and RQ-PCR. RNA extraction, reverse transcription (RT) and RQ-PCR were as described in Pillozzi *et al*, 2007. The primers relative to *ATP7A*, *ATP7B*, *KCNA3*, *KCNH1*, *KCNH2*, *KCNMA1*, *KCNN3*, *KCNN4*, *SLC31A1*, *SLC31A2*, *LRCC8A* and *LRCC8D* are shown in Supplementary Table S1.

Silencing of HCT-116 cells. Silencing of HCT-116 cells was carried out as in Crociani *et al*, 2013, using the following siRNAs: (1) K_v11.1/KCNH2-siRNAs (44858 anti-Kv11.1 siRNA1 and 44762 anti-Kv11.1 siRNA3, Ambion; Austin TX, USA) (total 100 nM final concentration) and (2) K_{Ca}3.1/KCNN4-siRNAs (7801 anti-kcnn4 siRNA1 and 7803 anti-kcnn4 siRNA3, Ambion) (total 5 nM final concentration). As negative controls, cells were treated with Lipofectamine only.

Cell viability assay, IC₅₀ and Combination Index (CI) calculation. Cell viability was measured through the Trypan Blue exclusion test, following the procedure described in Pillozzi *et al*, 2016. IC₅₀ and CI calculations are as in Pillozzi *et al*, 2011. Cells were seeded at 1 × 10⁴ per well in 96-well plates (Costar Corning, Cambridge, MA, USA) in complete medium; Cisplatin and the other drugs were added at their final concentration after 24 h incubation and further incubated for different times.

Cell cycle analysis. Cell cycle distribution was assessed by flow cytometry after staining cells with propidium iodide (PI) as in Pillozzi *et al*, 2016.

Annexin/PI assay. Apoptosis was determined using the Annexin V/PI test (Annexin-V FLUOS Staining Kit; Roche Diagnostics, Mannheim, Germany) as described in Pillozzi *et al*, 2011. According to this procedure, (i) viable cells are negative for both Annexin V and PI (Q3 quadrant gate in the dot plots); (ii) cells that are in the early phases of apoptosis are Annexin V positive and PI negative (Q4 quadrant gate in the dot plots); (iii) cells that are in the late phases of apoptosis are both Annexin V and PI positive (Q2 quadrant gate in the dot plots); and (iv) dead (necrotic) cells are Annexin V negative and PI positive (Q1 quadrant gate in the dot plots).

Patch-clamp experiments. Membrane currents were recorded at room temperature (25 °C) with the whole-cell configuration of the patch-clamp technique. K_v11.1 currents were elicited by a two-step protocol, conditioning the cell at 0 mV and testing the tail current at -120 mV (Gasparoli *et al*, 2015). K_{Ca}3.1 currents were elicited by 200-ms voltage ramps from -120 to +40 mV applied every 10 s,

and the fold increase of slope conductance by drug was taken as an indication of channel activation (Sankaranarayanan *et al*, 2009). All the solutions are mentioned in Supplementary Table S2. The effects of Riluzole, SKA-31 and Cisplatin were determined on maximal K_v11.1 tail currents. The effects of Cisplatin and TRAM-34 were determined on the maximal K_{Ca}3.1 activation induced by Riluzole and SKA-31. Drugs were applied at the concentrations indicated in the figure legends for 2 min before recording their effects. Resting potential (V_{REST}) values were measured in $I=0$ mode, in the presence of the extracellular solution No. 1 (see Supplementary Table S2).

Immunofluorescence. Immunofluorescence was performed applying the procedures detailed in Lastraioli *et al*, 2015, using the antibodies reported in Supplementary Methods.

Protein extraction and WB. Protein extraction and WBs relative to cell lines and tumour masses were performed as described in Crociani *et al*, 2013, using the antibodies reported in Supplementary Methods.

Cisplatin uptake measurement. HCT-116 cells were incubated in complete medium containing the different compounds as reported in the legend of Figure 4 for 3 or 24 h. For incubation in high extracellular K⁺, NaCl in the RPMI medium was substituted in part (to obtain 40 mM KCl) or totally (to obtain 108 mM KCl) with KCl. At the end of the uptake period, cells were quickly washed three times with ice-cold PBS, collected, gently spun down (1.000 g for 5 min at 4 °C), and the pellet suspended in 1 ml ice-cold PBS. Part (50 μ l) of this suspension was taken for protein concentration determination and part (50 μ l) for cell viability assay. The remaining 900 μ l were spun down at 400 g for 5 min and processed for ICP-AES analysis as described in Marzo *et al*, 2015.

In vivo experiments. Experiments were performed at the Animal House of the University of Florence (CESAL). Mice were housed in filter-top cages with a 12 h dark–light cycle and had unlimited access to food and water. Procedures were conducted according to the laws for experiments on live animals (Directive 2010/63/EU) and approved by the Italian Ministry of Health (1279/2015-PR). All the procedures are detailed in Supplementary Methods.

Statistical analysis. Unless otherwise indicated, data are given as mean values \pm s.e.m., with n indicating the number of independent experiments. Statistical comparisons were performed with OriginPro 2015 (Origin Lab, Northampton, MA, USA). The normality of data distribution was checked with Kolmogorov–Smirnov test. In case of unequal variances, the Welch correction was applied. For comparisons between two groups, we used Student's t -test. For multiple comparisons, one-way ANOVA followed by Bonferroni's *post hoc* test was performed to derive P -values. The individual P -values are reported in the Figures.

RESULTS

Effects of Cisplatin on different CRC cell lines: identification of Cisplatin-resistant and -sensitive cell lines. We investigated the response of four CRC cell lines (HCT-116, HCT-8, HT-29 and H-630) to Cisplatin treatment by measuring the cell viability by Trypan Blue exclusion test. The inhibiting concentration 50 (IC₅₀) values determined after 24 h of treatment (Figure 1A) show that HCT-116 cells are the most resistant and HCT-8 the most sensitive (see also Table 1A and Supplementary Table S3). Cisplatin, added at its IC₅₀ value to the two cell lines, triggered apoptosis (with a higher percentage of cells in late apoptosis in HCT-8 cells than in HCT-116 cells (Figure 1B, Table 1A) and increased the percentage of G0/G1 cells in both cell types (Table 1A and Supplementary Figure S1) after 24 h of treatment. Cisplatin blocked cell

proliferation in HCT-8 at 1 μ M (Figure 1C, left panel), while in HCT-116 at 20 μ M (Figure 1C, right panel). In summary, HCT-116 is a Cisplatin-resistant line, while HCT-8 is Cisplatin sensitive.

We next determined the expression of different K⁺ channel genes (Spitzner *et al*, 2007; D'Amico *et al*, 2013; Huang and Jan, 2014) and Cisplatin transporter systems (Owatari *et al*, 2007; Pedersen *et al*, 2015; Barresi *et al*, 2016; Jentsch *et al*, 2016) in the two CRC cell lines, focussing on those already reported to be expressed in CRC cells and primary samples. RQ-PCR data are shown in Figure 1D. K_v11.1 (KCNH2, hERG1) was expressed at higher levels in HCT-116 than HCT-8 cells. The K_{Ca}3.1 (KCNN4) transcript was also highly expressed in HCT-116 cells and much less so in HCT-8 cells. All other tested K⁺ channel transcripts were negligible in both cell lines. The copper transporter CTR1 (SLC31A1) was highly expressed in both cell lines; the two P-type ATPases, ATP7A (ATP7A) and ATP7B (ATP7B) displayed a higher amount in HCT-8 cells; the LRRC8A/D (LRCC8A and LRCC8D) components of VRAC were only found in HCT-116 cells.

The higher expression of both K_v11.1 (KCNH2, hERG1) and K_{Ca}3.1 (KCNN4) in HCT-116 compared with HCT-8 cells was confirmed by WB (Figure 1E), immunofluorescence (Figure 1F) and patch-clamp experiments. Larger K_v11.1 currents were previously reported in HCT-116 than in HCT-8 cells (Crociani *et al*, 2013, and Supplementary Figure S2). A calcium-activated K⁺ current with characteristics of K_{Ca}3.1 was detected only in HCT-116 cells but only after the channel was activated by Riluzole or SKA-31 (Figure 2A). HCT-116 cells showed a significantly hyperpolarised V_{REST} (-38.5 ± 2.9 mV, $n = 11$) compared with HCT-8 cells (-13.1 ± 2.5 mV, $n = 12$, $p < 0.01$), consistent with their higher expression of K⁺ channels.

Modulators of K_{Ca}3.1 and K_v11.1 channels affect viability, apoptosis and cell cycle phases of CRC cells. Next, we tested on our cell lines the effects of activators or inhibitors of K_{Ca}3.1 and inhibitors of K_v11.1. Riluzole was used as a broad modulator of ion channels, as it activates K_{Ca} currents (both intermediate-conductance K_{Ca}3.1 and small-conductance K_{Ca}2.1, K_{Ca}2.1 and K_{Ca}2.3 currents) and inhibits K_v11.1 (Sankaranarayanan *et al*, 2009), voltage-gated sodium (Wang *et al*, 2008) and voltage-gated calcium channels (Stefani *et al*, 1997). SKA-31 is a specific K_{Ca}3.1 activator (Sankaranarayanan *et al*, 2009) and TRAM-34 a specific K_{Ca}3.1 inhibitor (Wulff *et al*, 2000). E4031 inhibits K_v11.1 (Sanguinetti and Jurkiewicz (1990)). We first tested these compounds on HCT-116 cells. Both Riluzole and SKA-31 increased the K_{Ca}3.1 current (reversal potential at -80 mV; inhibition by TRAM-34) 2.11 ± 0.46 ($n = 9$) and 4.36 ± 1.67 ($n = 10$) fold, respectively (Figures 2A and C) and induced cell hyperpolarisation (Figure 2A). Riluzole also inhibited K_v11.1 currents (by 23 and 44%, with 10 and 45 μ M, respectively) (Figures 2B and C), in keeping with previous reports (Sankaranarayanan *et al*, 2009). SKA-31 had no effect on K_v11.1 currents (Figures 2B and C).

In current-clamp experiments, both Riluzole and SKA-31 strongly hyperpolarised V_{REST} (Figure 2E, right panel). In contrast, TRAM-34 (Figure 2D) and E4031 (Figure 2E) depolarised V_{REST} . Cisplatin did not significantly affect K_{Ca}3.1 currents either in control conditions or after SKA-31 stimulation (Figures 2B and F) and slightly inhibited K_v11.1 (Figures 2B and G). Cisplatin addition rapidly and reversibly depolarised V_{REST} (Figure 2H).

Next, we tested the effects of Riluzole, SKA-31, E4031 and TRAM-34 on cell viability, apoptosis and cell cycle phases of HCT-116 and HCT-8 cells. All these compounds reduced cell viability, but differently from Cisplatin, their IC₅₀ values were generally lower in HCT-116 than in HCT-8 cells, except for TRAM-34 (Table 1A and Supplementary Table S3). All the K⁺ channel modulators triggered apoptosis in HCT-116 cells, and the effect was smaller in HCT-8 cells (Table 1A). They also increased the percentage of cells in G0/G1 phase, in both cell lines, with the

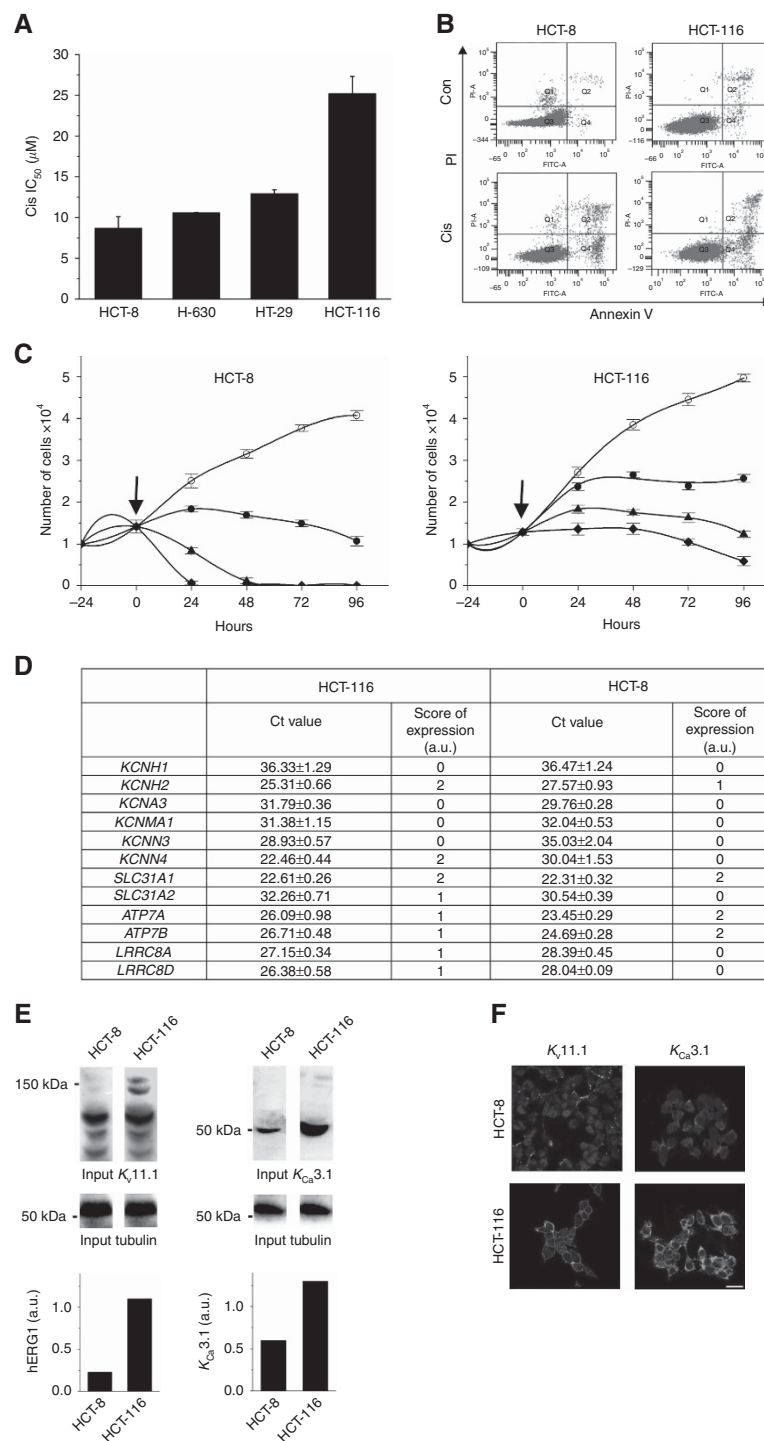


Figure 1. Effects of Cisplatin and characterisation of K⁺ channel expression in CRC cell lines. **(A)** IC₅₀ values of Cisplatin on different CRC cell lines. Cell viability was assessed after 24 h of treatment with Cisplatin (range 0–100 µM) by the Trypan Blue exclusion test. IC₅₀ values are means ± s.e.m. of four independent experiments. **(B)** Dot plots of Annexin/PI analysis of HCT-116 and HCT-8 cells treated (Cis) or not (Con) for 24 h with Cisplatin, at the IC₅₀ value of the two cell lines. Representative of three independent experiments. **(C)** Effects of different Cisplatin on proliferation (expressed as the number of live, Trypan Blue-negative cells) of HCT-8 and HCT-116 cells. Data are means ± s.e.m. of six independent experiments. Arrow = addition of the drug. White circle = control, black circle = Cisplatin 1 µM, black triangle = Cisplatin 10 µM, black rhombus = Cisplatin 20 µM. For statistical analysis, the one-way ANOVA was applied. **(D)** RQ-PCR of the transcripts of K⁺ channels and transporters in HCT-116 and HCT-8 cells (primer pairs are in Supplementary Table S1). Data are means ± s.e.m. of three experiments and are expressed as Ct values of the target gene. Ct values of the reference gene (*gapdh*) are 17.54 ± 0.90 for HCT-116 and 17.14 ± 0.22 for HCT-8. The score of expression is reported as arbitrary units (a.u.) and was calculated as follows: ≥28 Ct = 0 (no expression); <28 Ct > 25 Ct = 1 (expression); <25 Ct = 2 (high expression). The names of the ion channel/transporter encoding genes are based on the IUPHAR and HGNC nomenclatures. **(E)** Expression of K_v11.1 and K_{Ca}3.1 proteins in HCT-8 and HCT-116 cells evaluated by WB. The corresponding densitometric results are given in the bar graph. **(F)** Expression of K_v11.1 and K_{Ca}3.1 proteins in HCT-8 and HCT-116 cells evaluated by immunofluorescence. Representative fields of vision are shown taken from two independent experiments. Scale bar: 50 µm.

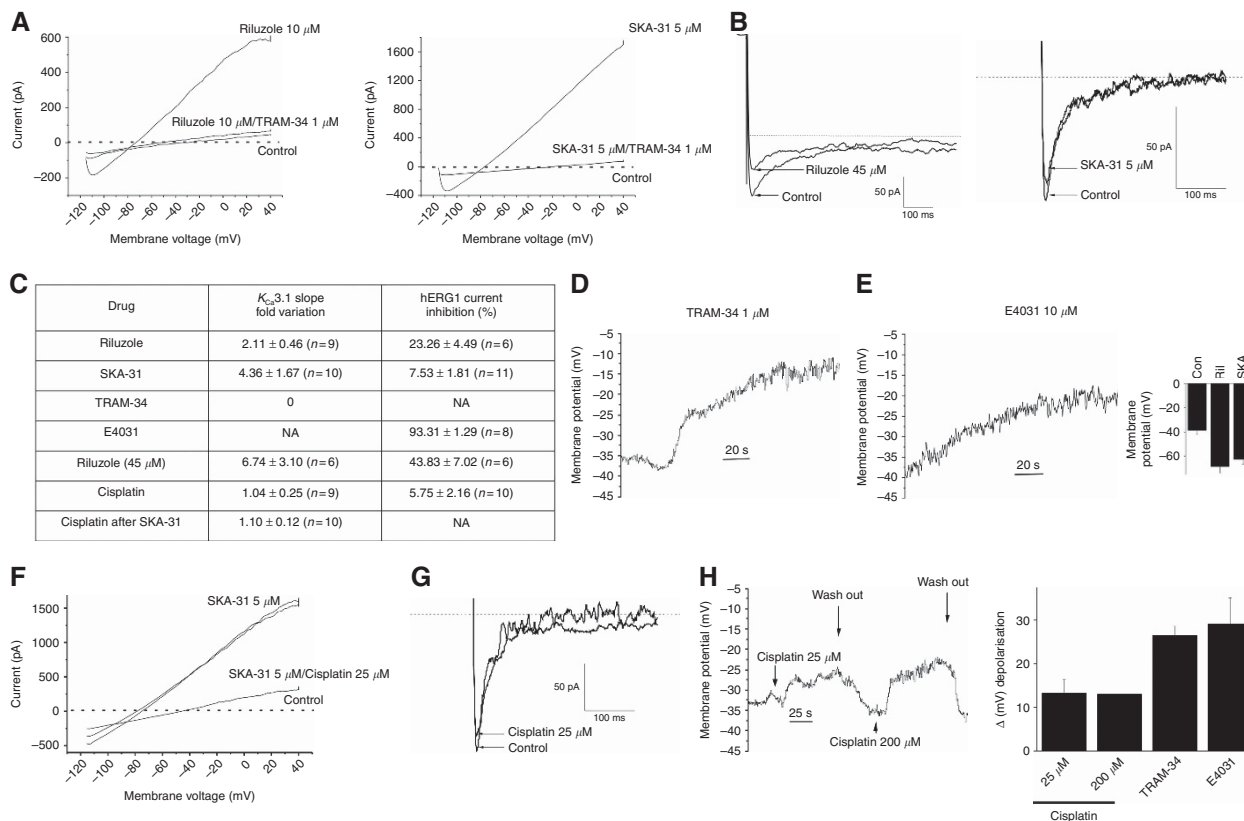


Figure 2. Effects of Riluzole, SKA-31, TRAM-34 and Cisplatin on K_{Ca}3.1 and K_v11.1/hERG1 currents in HCT-116 cells. **(A)** K_{Ca}3.1 currents in HCT-116 cells: effects of Riluzole and SKA-31 after 1 min of perfusion, and effects of TRAM-34 on elicited currents. The results are representative of 20 cells analysed in 5 different experiments. The dotted lines represent the zero value of the current (left and middle panels). **(B)** K_v11.1 currents in HCT-116 cells: effects of Riluzole and SKA-31 after 3 min of perfusion. Eight representative cells were analysed for Riluzole and 14 for SKA-31 in 3 different experiments. The dotted lines represent the zero value of the current. **(C)** Effects of Riluzole, SKA-31, TRAM-34, E4031 and Cisplatin on K_{Ca}3.1 and K_v11.1 (hERG1) currents of HCT-116 cells. Data are mean ± s.e.m. of data obtained in the number of cells shown in parenthesis, tested in three different experiments. For statistical analysis the Student's *t*-test was applied and individual *P*-values are reported in Supplementary Material. **(D)** Effect of TRAM-34 and of E4031 on the time course of V_{REST} of HCT-116 cells, measured in current-clamp mode. In both cases, five representative cells were analysed in three different experiments. **(E)** V_{REST} hyperpolarisation of HCT-116 cells produced by Riluzole and SKA-31 in current-clamp experiments. **(F)** Left panel. Effect of Cisplatin on SKA-31 elicited K_{Ca}3.1 currents in HCT-116 cells. Eight representative cells were analysed in three different experiments. Right panel. Effect of Cisplatin on K_v11.1 currents in HCT-116 cells. Ten representative cells were analysed in three different experiments. The dotted line represents the zero value of the current. **(G)** Effect of Cisplatin (25 and 200 μM) on the time course of V_{REST} of HCT-116 cells, measured in current-clamp mode. Five representative cells were analysed in two different experiments. **(H)** Δ (mV) depolarisation of the HCT-116 cells V_{REST} induced by Cisplatin, TRAM-34 or E4031 in current-clamp experiments. Unless otherwise indicated in the figure, the drugs were used at the following doses: Riluzole 10 μM, SKA-31 5 μM, TRAM-34 1 μM, E4031 10 μM, Cisplatin 25 μM.

exception of Riluzole, which caused a strong G2/M block in HCT-8 cells (Table 1A), as reported by Khan *et al* (2011). All drugs reduced HCT-116 cell proliferation when added at time zero at their specific IC₅₀ values (Figure 3A). Less evident effects were observed in HCT-8 cells (Supplementary Figure S3).

K_{Ca}3.1 activation and K_v11.1 block have a synergistic activity with the pro-apoptotic effects of Cisplatin. We tested the different K⁺ channels modulators in combination with Cisplatin in HCT-116 and HCT-8 cells and measured the CI to assess synergistic, antagonistic or additive effects of the different combinations (Pillozzi *et al*, 2011). Riluzole, SKA-31 and E4031 synergised with Cisplatin in decreasing viability of HCT-116 cells after a 24 h incubation, whereas TRAM-34 was antagonistic (Table 1B and Figure 3B and Supplementary Table S4). A synergistic effect of Riluzole, SKA-31 and E4031 was also observed with Oxaliplatin (Table 1B and Supplementary Table S6), which was weakly efficacious when tested alone on HCT-116 cells (Table 1A). All drugs increased the pro-apoptotic effect of Cisplatin in HCT-116 cells (Table 1B), while the effects of the

combination treatments on cell cycle were less homogeneous (Supplementary Table S7). TRAM-34, which was antagonistic in HCT-116 cells, only slightly increased the percentage of cells in early apoptosis and the percentage of cells in G2/M (Supplementary Table S7). In HCT-8 cells, all the K⁺ channel modulators were antagonistic to Cisplatin (Supplementary Table S5) and decreased apoptosis (Supplementary Table S8).

Next, we studied the signalling pathways underlying such effects, focussing on Caspase 3 activation and the inhibition of antiapoptotic molecules, such as ERK1/2 and Akt (Wong, 2011). Cisplatin activated Caspase 3, with no or only a small effect on ERK and Akt phosphorylation. The combination of Cisplatin with K_{Ca}3.1 activators (Riluzole or SKA-31) further activated Caspase 3 and reduced Akt phosphorylation, without affecting the ERK1/2 pathway. Cisplatin and TRAM-34 decreased ERK1/2 phosphorylation and increased Caspase 3 activation but did not affect Akt phosphorylation. The combination of Cisplatin with E4031 strongly decreased ERK1/2 and Akt phosphorylation and activated Caspase 3 (Figure 3C). Overall, the synergistic pro-apoptotic effects of Cisplatin with Riluzole, SKA-31 and E4031 were mediated by

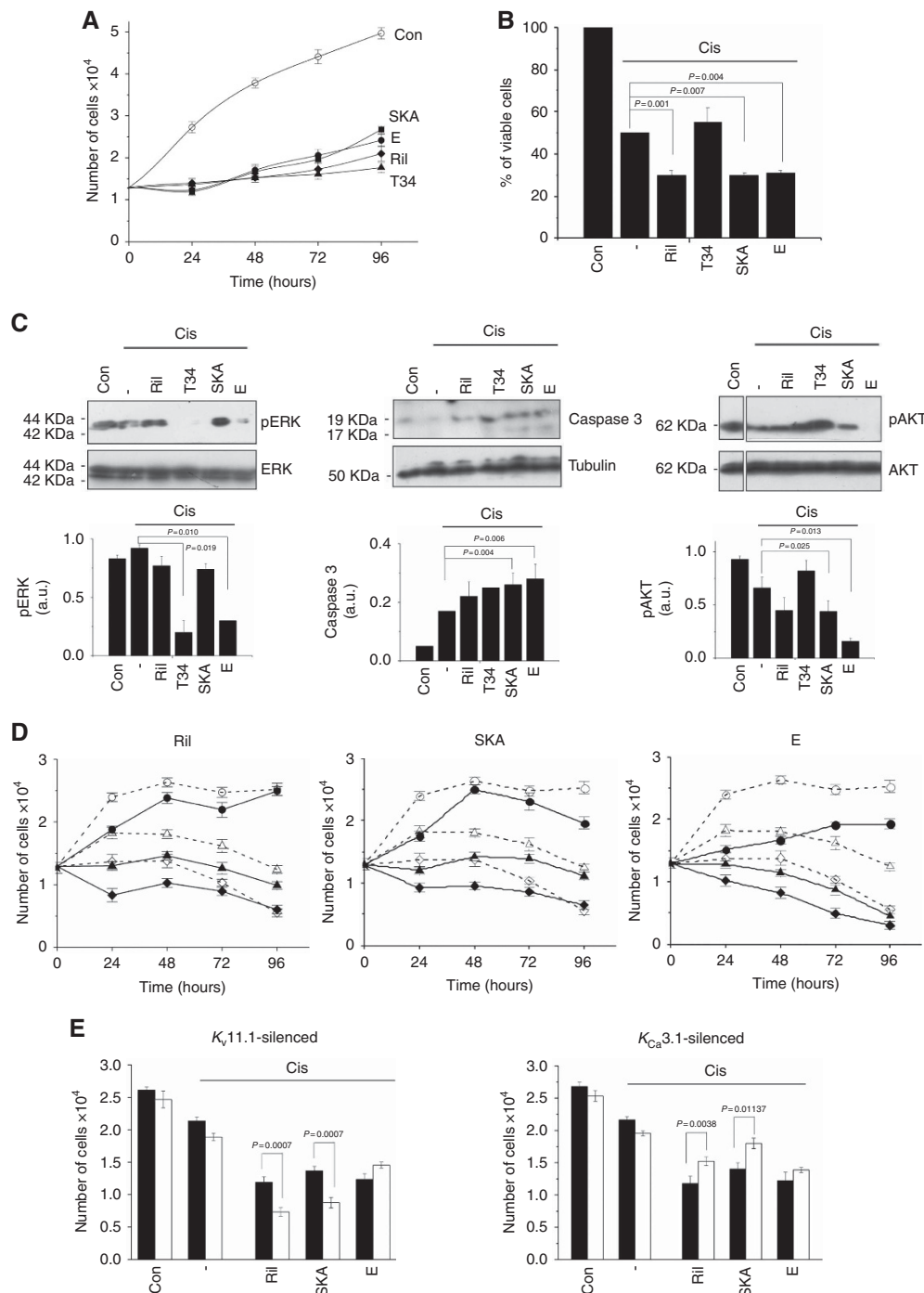


Figure 3. Effects of Riluzole (Ril), SKA-31 (SKA), E4031 (E) and TRAM-34 (T34) on proliferation of HCT-116 cells. **(A)** Effects of Riluzole, SKA-31, E4031 and TRAM-34 on proliferation of HCT-116 cells after a single treatment. Drugs were added 24 h after cell seeding, indicated as time 0 in the figure. Data are given as the number of Trypan Blue-negative cells. Data are means \pm s.e.m. of three independent experiments. **(B)** Cell viability after 24 h of treatment with Cisplatin in combination with Riluzole, SKA-31, E4031 and TRAM-34. Data are means \pm s.e.m. of four independent experiments. **(C)** WB analysis of the protein levels of p-ERK1/2^{Thr202/Tyr204} (42/44 KDa), p-Akt^{Thr308} (62 KDa) and Caspase 3 (19–17 KDa) in HCT-116 cells treated for 24 h with Cisplatin alone or in combination with Riluzole, TRAM-34, SKA-31 and E4031. The membranes were then reprobated with an anti-ERK1/2, anti-Akt or anti-tubulin antibody. Representative of three independent experiments; the corresponding densitometric results are given in the bar graph. *P*-values were calculated with respect to Cisplatin-treated cells, by Student's *t* test. **(D)** Effects of different Cisplatin on proliferation (expressed as the number of live, Trypan Blue-negative cells) of HCT-8 and HCT-116 cells. Data are means \pm s.e.m. of six independent experiments. Arrow = addition of the drug. White circle = control, black circle = Cisplatin 1 μ M, black triangle = Cisplatin 10 μ M, black rhombus = Cisplatin 20 μ M. For statistical analysis, the one-way ANOVA was applied. **(E)** Effects of Cisplatin in combination with Riluzole, SKA-31 and E4031 on HCT-116 cell proliferation. Drugs were added after 24 h of cell seeding, indicated as time 0 in the figure. Data are given as the number of Trypan Blue-negative cells. Data are means \pm s.e.m. of three independent experiments. White circle = Cisplatin 1 μ M, white triangle = Cisplatin 10 μ M, white rhombus = Cisplatin 20 μ M; black circle = Cisplatin 1 μ M + IC50 of the relative combined drug, black triangle = Cisplatin 10 μ M + IC50 of the relative combined drug; black rhombus = Cisplatin 20 μ M + IC50 of the relative combined drug. Statistical analysis was performed by Student's *t*-test and *P*-values are reported in Supplementary Material.

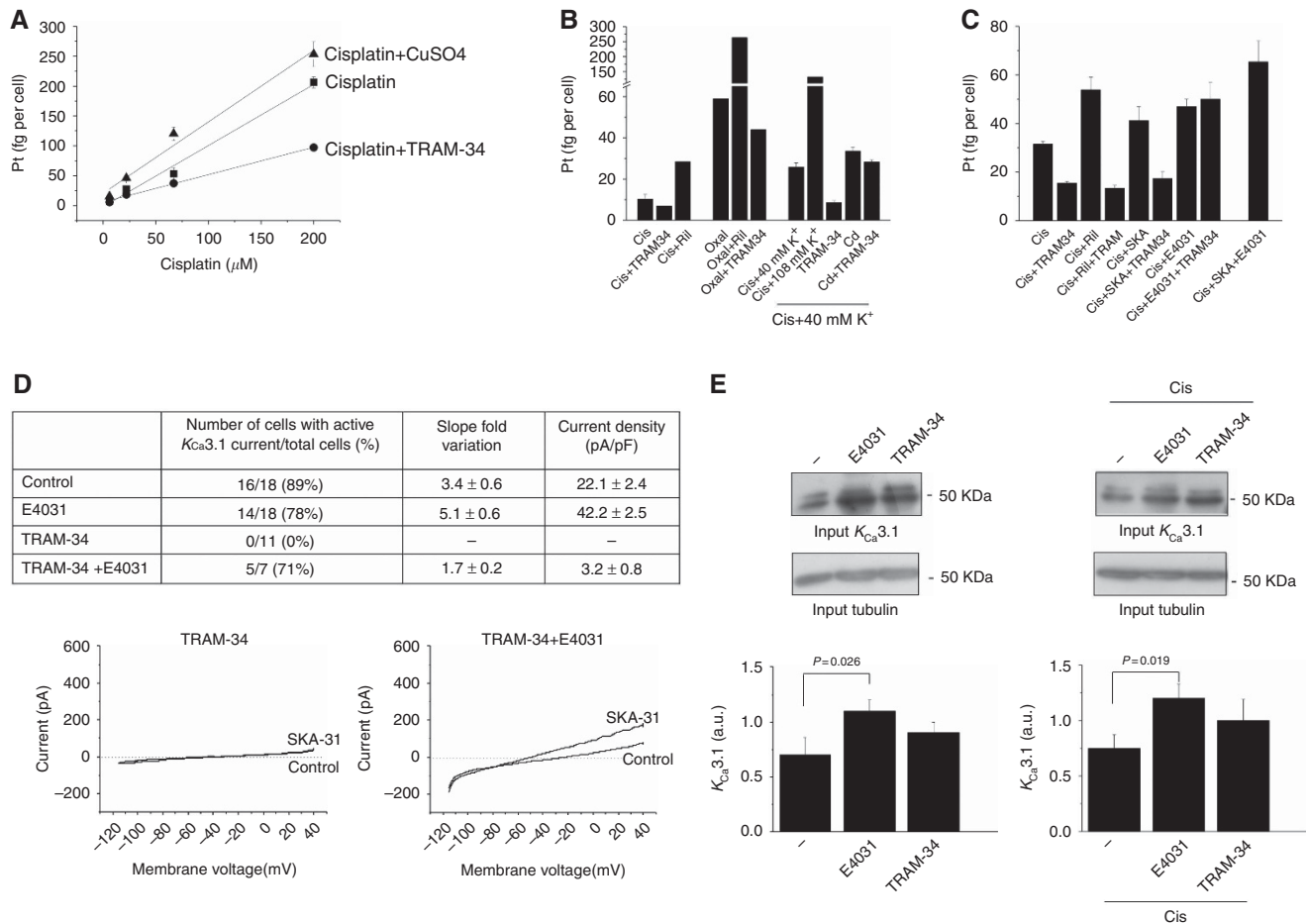


Figure 4. Effect of K⁺ channel modulators on Cisplatin uptake in HCT-116 cells. **(A)** Platinum (Pt) uptake (measured as fg per cell) after 3 h of treatment with Cisplatin at different concentrations, alone and in combination with CuSO₄ or TRAM-34. **(B)** Pt uptake after 3 h of treatment with Cisplatin (25 μM) or Oxaliplatin (60 μM, i.e. the respective IC₅₀ values) in standard medium or in medium with 40 or 108 mM K⁺ alone and in combination with Riluzole, TRAM-34 (at their respective IC₅₀ values) or Cd²⁺ (200 μM). Data are means ± s.e.m. (or values of single experiment) of the number of independent experiments shown in the figure. **(C)** Pt uptake after 24 h of treatment with Cisplatin (at the IC₅₀ value) alone and in combination with SKA-31, TRAM-34, E4031 and Riluzole at their respective IC₅₀ values. Data are means ± s.e.m. of the number of independent experiments shown in the figure. **(D)** Analysis of slope fold variation and current density after treatment for 24 h with E4031, TRAM-34 (1 μM) or E4031 + TRAM-34. The current traces in the below panel show the maximal activation of K_{Ca}3.1 currents by SKA-31 after 24 h incubation with TRAM-34 or TRAM-34 plus E4031. **(E)** K_{Ca}3.1 protein expression in HCT-116 cells treated for 24 h with E4031 or TRAM-34 alone or in combination with Cisplatin. All drugs were used at the respective IC₅₀ values. Cell lysates from HCT-116 cells were blotted and probed with the anti-K_{Ca}3.1 antibody. Reprobing of membranes with anti-tubulin antibody is reported in the bottom panels. Representative of three independent experiments. The corresponding densitometric results are given in the bar graph.

both the Akt and Caspase 3 pathways. E4031 also modulated the MAPK pathway. Cisplatin and TRAM-34 were antagonistic because of a lack of convergence on the Akt pathway, which could impair completing the apoptotic process (see the relatively low percentage of cells in late apoptosis observed in cells treated with Cisplatin and TRAM-34 in Table 1B).

Riluzole, SKA-31 and E4031 had a synergic effect with Cisplatin also on the inhibition of HCT-116 cell proliferation. This effect was particularly evident with low Cisplatin concentrations, and the strongest effect was obtained with E4031 (Figure 3D).

We then studied whether the antiproliferative effects and the synergy with Cisplatin of drugs that activate K_{Ca}3.1 (Riluzole, SKA-31) or inhibit K_v11.1 (E4031) depended on their effects on either K_{Ca}3.1 or K_v11.1 currents. Hence the drugs were tested in K_v11.1- and K_{Ca}3.1-silenced HCT-116 cells. The silencing of K_v11.1 and K_{Ca}3.1 by specific siRNAs is shown in Supplementary Figure S4. Silencing K_v11.1 potentiated the Cisplatin effects in combination with Riluzole or SKA-31 while it abrogated the effects of E4031 (Figure 3E, left panel). Conversely, silencing K_{Ca}3.1

reversed the effects of both Riluzole and SKA-31 (Figure 3E, right panel). We conclude that specific activation of K_{Ca}3.1 and/or inhibition of K_v11.1 underlie the synergistic antiproliferative effects of Riluzole, SKA-31 or E4031 in combination with Cisplatin.

K⁺ channel modulators increase Cisplatin uptake in CRC cells. We next tested whether Riluzole, SKA-31 or E4031 affected Cisplatin uptake, measured as intracellular accumulation of Platinum (Pt), in HCT-116 cells. We first analysed the role of Cu transporters, determining the dose dependence of Cisplatin accumulation in the absence or presence of 1 mM CuSO₄ to inhibit Cu transporters (Matsumoto *et al*, 2007). Unexpectedly, CuSO₄ had no effect. Hence, Cu transporters do not have a significant role in the intracellular accumulation of Cisplatin in these cells. The same experiment was performed in the presence of 25 μM TRAM-34, a dose that fully inhibits K_{Ca}3.1, without affecting cell viability after a 3 h incubation (Supplementary Figure S5A). Blocking K_{Ca}3.1 channels reduced Cisplatin uptake (Figure 4A). This result was confirmed by incubating the cells for 3 h with the IC₅₀ dose

Table 1A. IC₅₀ values and effects on apoptosis and cell cycle distribution of Cisplatin, Riluzole, SKA-31, TRAM-34 and E4031 in HCT-116 and HCT-8 cells

			Apoptosis		Cell cycle		
	IC ₅₀ (μM)	Concentration of the drug (μM)	Early apoptosis (%)	Late apoptosis (%)	G0/G1 (%)	S (%)	G2/M (%)
HCT-116							
Control	—		1.0 ± 0.6	0.8 ± 0.5	27.7 ± 7.7	55.5 ± 3.7	16.9 ± 6.4
Cisplatin	25.2 ± 2.1	25	5.9 ± 1.0 P=0.001	5.3 ± 1.5 P=0.009	48.0 ± 4.5 P=0.009	39.2 ± 2.5 P=0.018	12.8 ± 3.3
Riluzole	9.5 ± 1.0	10	13.6 ± 3.7 P=0.004	10.3 ± 4.1 P=0.028	51.6 ± 6.0 P=0.004	26.1 ± 8.8 P=0.021	22.3 ± 3.1
SKA-31	5.3 ± 0.3	5	7.0 ± 0.9 P=0.000	3.5 ± 0.9 P=0.015	55.3 ± 2.4 P=0.006	31.4 ± 7.7 P=0.028	13.3 ± 5.7
TRAM-34	24.4 ± 1.8	25	9.6 ± 2.1 P=0.001	6.6 ± 0.9 P=0.000	50.5 ± 3.2	34.2 ± 5.0	15.4 ± 7.6
E4031	6.6 ± 1.6	7	5.2 ± 1.2 P=0.005	4.1 ± 1.0 P=0.010	51.4 ± 4.3 P=0.010	26.4 ± 4.1 P=0.012	22.3 ± 6.1
HCT-8							
Control	—		0.8 ± 0.3	1.2 ± 0.3	30.7 ± 2.4	53.8 ± 3.3	15.5 ± 1.9
Cisplatin	8.7 ± 1.4	9	5.5 ± 1.4 P=0.008	13.4 ± 7.2 P=0.018	46.9 ± 1.3 P=0.019	43.4 ± 1.9 P=0.002	9.7 ± 3.1 P=0.041
Riluzole	12.9 ± 0.7	13	3.6 ± 0.9 P=0.008	4.0 ± 1.2 P=0.035	8.5 ± 3.4 P=0.003	6.7 ± 4.3 P=0.000	84.6 ± 5.6 P=0.000
SKA-31	46.9 ± 1.4	45	3.0 ± 0.4 P=0.001	10.2 ± 5.0 P=0.011	47.5 ± 3.4 P=0.021	39.9 ± 8.7 P=0.046	12.6 ± 10.0
TRAM-34	20.1 ± 1.1	20	3.2 ± 1.2 P=0.012	2.7 ± 1.0 P=0.019	62.9 ± 3.2 P=0.026	28.9 ± 4.5 P=0.026	8.2 ± 7.6
E4031	13.3 ± 1.3	13	2.8 ± 1.9	2.8 ± 0.7 P=0.015	25.2 ± 0.4 P=0.012	57.1 ± 2.2	17.7 ± 2.4

IC₅₀ values were determined after 24 h of treatment by the Trypan Blue exclusion test, using the Origin Software. Apoptosis and cell cycle distributions were evaluated by treating the cells with the drug concentrations indicated in the third column for 24 h. The percentage of cells in early (Annexin +/PI - cells) and late apoptosis (Annexin +/PI + cells) was determined by Annexin/PI assay as detailed in the Materials and Methods section. Cell cycle distribution was assessed by flow cytometry after staining the cells with propidium iodide (PI) and is indicated as the percentage of cells in the different cell cycle phases. Data are means ± s.e.m. of three independent experiments, each carried out in triplicate. For statistical analysis, Student's t-test was applied.

(22 μM) of Cisplatin (Figure 4B). Hence, the activity of K_{Ca}3.1 channels determines or at least contributes to the uptake of Cisplatin in HCT-116 cells. Consistently, Riluzole increased Cisplatin accumulation (Figure 4B). A similar mechanism was observed for Oxaliplatin uptake (Figure 4B). Recalling the opposing effects of TRAM-34 (depolarisation) and Riluzole (hyperpolarisation) on V_{REST} of HCT-116 cells (Figure 2), we also evaluated the effect of membrane depolarisation on Cisplatin uptake. Cells were depolarised by exposure to a high K⁺ medium (either 40 or 108 mM), which increased Pt uptake. The effect depended on K_{Ca}3.1 activity (as it was reduced by TRAM-34) but not on Ca²⁺ influx through voltage-gated Ca²⁺ channels (as 200 μM CdCl₂ had no effect; Becchetti *et al*, 1992).

Cisplatin uptake was then determined after longer (24 h) treatment with Cisplatin (at the IC₅₀ dose), alone or in combination with our K⁺ current modulators. Riluzole, SKA-31 and E4031 increased, while TRAM-34 decreased, Cisplatin accumulation (Figure 4C). TRAM-34 inhibited the potentiation of Cisplatin uptake induced by SKA-31 or Riluzole, while it did not affect the potentiation by E4031. Finally, the combination of SKA-31 and E4031 induced the largest increase in Cisplatin uptake (Figure 4C). These data suggest that Cisplatin uptake in HCT-116 cells is facilitated by K_{Ca}3.1 channels, being increased by their activation and reduced by their inhibition.

To determine why K_v11.1 inhibition alone increased Cisplatin uptake, we examined whether K_v11.1 activity was related to K_{Ca}3.1 expression and/or activity. K_{Ca}3.1 channel activity (Figure 4D) and expression (Figure 4E) were analysed in HCT-116 cells treated for 24 h with E4031. Treatment with TRAM-34 was included as a control. E4031 augmented both K_{Ca}3.1 current amplitude (Figure 4D) and membrane expression (Figure 4E), both when it was applied alone and in the presence of Cisplatin (Figure 4E). TRAM-34 blocked K_{Ca}3.1 activity, as expected (Figure 4D), but

scarcely affected its surface expression (Figure 4E). Neither TRAM-34, nor E4031 altered K_v11.1 expression (Supplementary Figure S5B). Hence, in HCT-116 cells, inhibition of K_v11.1 currents was compensated by the increased expression of K_{Ca}3.1. TRAM-34 (25 μM) did not completely block K_{Ca}3.1 currents in E4031-treated cells (Figure 4D), as it did not completely block Cisplatin uptake in E4031-treated cells (Figure 4C). Overall, we attribute the increase in Cisplatin uptake in the presence of K_v11.1 inhibitors to the upregulation of K_{Ca}3.1 currents less sensitive to TRAM-34 inhibition, possibly a splice variant or a posttranslationally modified form (see Discussion section).

K⁺ channel modulators overcome Cisplatin resistance

in vivo. We next hypothesised that combining a K_{Ca}3.1 activator and a K_v11.1 inhibitor could potentiate the effect of low doses of Cisplatin (1 μM). Using Cisplatin in the presence of SKA-31, or E4031, or a compound with both effects (Riluzole) reduced cell viability to a greater extent than observed with each compound alone (Figure 5A). The most effective combination was Cisplatin + Riluzole + E4031 (see also the CI in Table 1B; note that both Riluzole and E4031 are K_v11.1 inhibitors, and their effects are likely to be additive, Figure 2C).

Finally, we tested whether the above synergistic effects also occurred in a preclinical *in vivo* model of chemoresistance. HCT-116 cells were xenografted subcutaneously into immunodeficient nude mice. Both Cisplatin (0.35 mg kg⁻¹, twice a week) and Riluzole (10 mg kg⁻¹, daily) reduced HCT-116 tumour growth, when added as single agents (Figure 5B and inset). The inhibitory effects of E4031 on tumour growth in the same mouse model have already been reported (Crociani *et al*, 2013). Moreover, we tested Riluzole and E4031 in a mouse model we have developed to mimic chemoresistance (see Supplementary Materials and Methods). To this purpose, xenografted mice were first treated with Cisplatin

(0.35 mg kg⁻¹, twice a week) for 1 week (Phase 1) and then with a 10 times lower dose (0.035 mg kg⁻¹) for a further 2 weeks (Phase 2). During Phase 2, Riluzole + E4031 were included in the treatment schedule (see the scheme in Figure 5C). Tumours decreased their growth by Cisplatin treatment during Phase 1 but recovered their growth during Cisplatin treatment in Phase 2, with approximately the same rate as displayed by the controls. In contrast, when both Riluzole and E4031 were included in the treatment schedule of Phase 2, both the growth rate and the final volume of tumours were significantly reduced (Figure 5C). Consistently, such treatment induced a strong decrease of ERK1/

2 and Akt phosphorylation and an increased activation of caspase 3 (Figure 5D).

DISCUSSION

In search of novel strategies to overcome Cisplatin resistance in CRC, we tested the effects of K⁺ channel modulators in combination with Cisplatin. We show that compounds that activate K_{Ca}3.1 (SKA-31) or inhibit K_v11.1 (E4031) or have both effects (Riluzole) promote Cisplatin uptake and enhance apoptosis of Cisplatin-resistant cells both *in vitro* and in a preclinical mouse model. Our results highlight the translational potential of using K⁺ channel modulators to overcome Cisplatin resistance in CRC.

Among the different K⁺ channel-encoding gene tested, Cisplatin-resistant (HCT-116) cells exhibited higher functional expression of K_{Ca}3.1 and K_v11.1 (hERG1, KCNH2) channels, compared with Cisplatin-sensitive HCT-8 cells. Moreover, the two channels are functionally related in these cells: (1) they set V_{REST} in HCT-116 cells to more hyperpolarised (−38.5 vs −13 mV) values compared with HCT-8 cells; and (2) their expression is coordinated in HCT-116 cells, one compensating for the other. In fact, prolonged (24 h) inhibition of K_v11.1 currents leads to upregulation of functional K_{Ca}3.1 channels (Figure 4D and E). As all described CRC cell lines express K_v11.1 (D'Amico *et al*, 2013) and K_{Ca}3.1 inhibition has no effect on K_v11.1 (Supplementary Figure S5B), we hypothesise that K_v11.1 drives the expression of the other K⁺ channel. The coordinated and balanced expression of the two K⁺ channels has two consequences in HCT-116 cells: (A) blocking K_v11.1 increases the uptake of Cisplatin, which relies on the activity of K_{Ca}3.1 channels, and (B) the concomitant activation of K_{Ca}3.1 and inhibition of K_v11.1 potentiates the pro-apoptotic activity of Cisplatin. Cisplatin uptake into HCT-116 cells is reduced by TRAM-34, a specific K_{Ca}3.1 blocker, and it is increased by SKA-31 and Riluzole, which activate K_{Ca}3.1. These results suggest a requirement for K_{Ca}3.1 in Cisplatin uptake. Blocking K_v11.1 (hERG1) with E4031 also enhances Cisplatin uptake, an effect that can be explained by E4031-induced upregulation of K_{Ca}3.1 (Table 2). Notably, the K_{Ca}3.1 upregulation triggered by E4031 is not completely blocked by TRAM-34. This decreased TRAM-34 sensitivity may be due to upregulation of a posttranslationally modified K_{Ca}3.1 protein (see K_{Ca}3.1 band of higher molecular weight, that is, more glycosylated, in Figure 4D) or a K_{Ca}3.1 splice variant with reduced TRAM-34 sensitivity as reported in the rat colon (Barmeyer *et al*, 2010). This could also explain why increased Cisplatin uptake in cells treated with E4031 was not completely reversed by TRAM-34 addition.

Moreover, the inhibitory effect of TRAM-34 was not related to its depolarising action. In fact, exposing the cells to high

Table 1B. Combination index and percentage (%) of apoptotic HCT-116 cells after different treatment combinations

Drug (concentration μM)	Combination index at IC ₅₀	Effect	Apoptosis	
			Early apoptotic cells (%)	Late apoptotic cells (%)
Cisplatin (25)	—		5.9 ± 1.0	5.3 ± 1.5
Cisplatin (25) + Riluzole (10)	0.70 ± 0.08	S	10.6 ± 1.3 P=0.021	17.6 ± 3.3 P=0.016
Cisplatin (25) + SKA-31 (5)	0.64 ± 0.11	S	12.5 ± 3.9	10.1 ± 2.4
Cisplatin (25) + TRAM-34 (25)	2.66 ± 0.78	A	13.8 ± 3.6 P=0.016	8.7 ± 1.6
Cisplatin (25) + E4031 (7)	0.68 ± 0.07	S	8.0 ± 0.3	13.2 ± 3.4 P=0.042
Cisplatin (25) + Riluzole (10) + E4031 (7)	0.47 ± 0.05	S	ND	ND
Cisplatin (25) + SKA-31 (5) + E4031 (7)	0.69 ± 0.14	S	ND	ND
Oxaliplatin (60) + Riluzole (10)	0.98 ± 0.01	S	ND	ND
Oxaliplatin (60) + SKA-31 (5)	0.71 ± 0.05	S	ND	ND
Oxaliplatin (60) + TRAM-34 (25)	3.36 ± 0.34	A	ND	ND
Oxaliplatin (60) + E4031 (7)	0.83 ± 0.01	S	ND	ND

Abbreviation: ND = not determined. CI > 1, antagonism (A); CI = 1, additivity (Ad); CI < 1, synergy (S). HCT-116 cells were exposed to Cisplatin or Oxaliplatin in combination with Riluzole, SKA-31, TRAM-34 and E4031 for 24 h as described in Pillozzi *et al*, 2011. All the drugs were used at drug concentrations indicated in the first column. Data are means ± s.e.m. of three independent experiments, each carried out in triplicate. CI values were calculated using the Calcsyn software Version 2 (Biosoft). For statistical analysis, Student's t-test was applied.

Table 2. Summary of the effects of K⁺ channel modulators (Riluzole, SKA-31, TRAM-34 and E4031) on different biological processes of HCT-116 cells

Drug	V _{REST}	Cisplatin			
		Platinum uptake	Cell viability	Apoptosis	Cell cycle
Riluzole	Hyperpolarisation	↑	↓ (S)	↑↑	↑↑ % of cells in G2/M
SKA-31	Hyperpolarisation	↑	↓ (S)	↑↑	↑ % of cells in G2/M
TRAM-34	Depolarisation	↓	(A)	↑↑	↑↑ % of cells in G2/M
E4031	Depolarisation	↑	↓ (S)	↑↑	↑ % of cells in G2/M

Abbreviations: ↓ = decrease, ↑ = increase, ↑↑ = strong increase, (A) = antagonism, (S) = synergy. V_{REST} was determined in cells treated with the single K⁺ channel modulators alone; Platinum uptake, cell viability, apoptosis and cell cycle data are relative to treatments in combination with Cisplatin (25 μM). Experimental data and concentrations used are from Table 1B, Figures 2–4 and Supplementary Table S7.

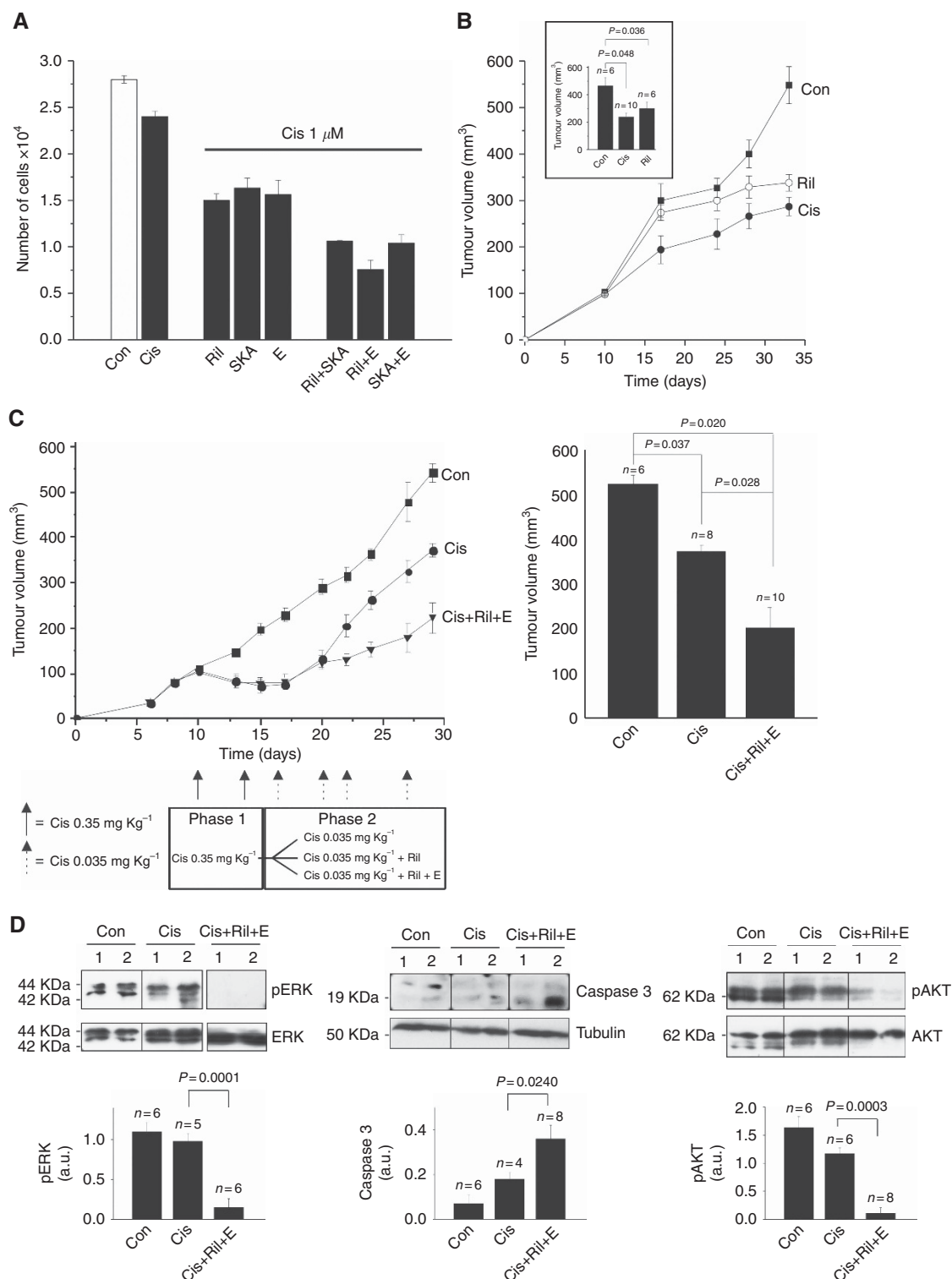


Figure 5. $K_{Ca3.1}$ activation and $K_{V11.1}$ block cooperate with Cisplatin *in vitro* and *in vivo*. **(A)** Effects of combined treatment with Cisplatin ($1 \mu\text{M}$), alone or in combination with Riluzole, SKA-31 or E4031 at their respective IC_{50} values. Data are reported as in Figure 3 and are means \pm s.e.m. of three independent experiments. **(B)** Time course of tumour growth in control, Cisplatin (0.35 mg kg^{-1}) and Riluzole (10 mg kg^{-1}) treated nude mice, subcutaneously injected with HCT-116 cells (3×10^6). Inset: volume of tumour masses at the killing. Data are reported as the mean \pm s.e.m. of the number of masses shown in the figure. Statistical analysis was performed by one-way ANOVA. **(C)** Left panel: Time course of tumour growth in control, Cisplatin-, Cisplatin + Riluzole- and Cisplatin + Riluzole + E4031-treated mice. Cisplatin was administered at 0.35 mg kg^{-1} for the first week and then lowered to 0.035 mg kg^{-1} for the following 2 weeks to mimic resistance (see scheme of treatment on the bottom). The slopes of the curves were: Cisplatin = 0.056 ; Cisplatin + Riluzole = 0.036 ; Cisplatin + Riluzole + E4031 = 0.033 . Right panel: Volume of tumour masses was measured at killing and calculated by applying the ellipsoid equation. Data are reported as the mean \pm s.e.m. of the number of masses shown in the Figure. Statistical analysis was performed by one-way ANOVA. **(D)** WB analysis of the protein levels of p-ERK1/2^{Thr202/Tyr204} (42/44 KDa), p-Akt^{Thr308} (62 KDa) and Caspase 3 (19–17 KDa) in tumour masses (the number of masses analysed is reported on the top of the bars) obtained from the injection of HCT-116 cells in nude mice. The membranes were then reprobbed with an anti-ERK1/2, anti-Akt or anti-tubulin antibody. The corresponding densitometric results are given in the bar graph. *P*-values were calculated with respect to the mice treated with Cisplatin, one-way ANOVA.

extracellular K⁺ concentrations (40 and 108 mM, which set V_{REST} at -10 and 0 mV, respectively) increased Cisplatin uptake. One possibility to explain this effect is that $K_{\text{Ca}3.1}$ modulates VRAC, which was found to mediate Cisplatin uptake (Jentsch *et al*, 2016). HCT-116 cells do show a substantial expression of *LRRc8D*, the main molecular component of VRAC implicated in cell volume regulation (Planells-Cases *et al*, 2015; Syeda *et al*, 2016). In this case, Cisplatin uptake through VRAC would be modulated by the activity of $K_{\text{Ca}3.1}$. Another possibility is that the depolarisation caused by high extracellular K⁺ also decreases the driving force for Cl⁻, leading to a smaller ratio between the outward and the inward flux. The consequent relative increase of inward Cl⁻ flux would facilitate Pt entry, compared with the basal conditions.

In Cisplatin-resistant CRC cells, $K_{\text{Ca}3.1}$ activators (SKA-31), $K_{\text{v}11.1}$ inhibitors (E4031) and compounds with both activities (Riluzole) displayed a synergistic action with Cisplatin. In fact, they restored the pro-apoptotic and cytotoxic effects of Cisplatin, even when the latter was tested at very low doses. The effect of E4031 in CRC cells is the opposite of that observed after silencing $K_{\text{v}11.1}$ /hERG1 in gastric cancer cells (Zhang *et al*, 2012), suggesting that different channel-dependent mechanisms are operant in CRC cells. The effects of our K⁺ channel-modulating drugs on apoptosis and cell cycle phases were generally stronger in Cisplatin-resistant cells. Moreover, in these cells, only $K_{\text{Ca}3.1}$ activators and $K_{\text{v}11.1}$ inhibitors were synergistic with Cisplatin, thus increasing the percentage of apoptotic cells, and affecting the relative intracellular signalling pathways (Table 2).

Although we studied mainly Cisplatin, the effects we observed were also evident with Oxaliplatin, stressing the translatability of our data. Overall, we believe that the results discussed herein may be of relevance for overcoming chemoresistance to Pt-based drugs, one of the major challenges in cancer treatment (Kartalou and Essigmann, 2001; Siddik, 2003; Wang and Lippard, 2005).

In our CRC model, HCT-116 cells, although expressing $K_{\text{Ca}3.1}$, have a low Cisplatin uptake because the activity of $K_{\text{Ca}3.1}$ is kept low by the concomitant $K_{\text{v}11.1}$ activity. The combination of $K_{\text{Ca}3.1}$ activation with $K_{\text{v}11.1}$ inhibition, improving Cisplatin uptake, allows also low doses of the drug to trigger apoptosis and reduce HCT-116 cell growth. This interpretation explains why a $K_{\text{Ca}3.1}$ activator and a $K_{\text{v}11.1}$ inhibitor can be combined to trigger a cooperative effect with Cisplatin. The best combination includes Riluzole, which has a mild $K_{\text{v}11.1}$ inhibitory activity, besides activating $K_{\text{Ca}3.1}$. In the present paper, we provide evidence that such cooperation occurs both *in vitro* and *in vivo* and in preclinical models (subcutaneous xenografts of HCT-116 cells into immunodeficient mice) and contributes to overcome Cisplatin resistance. In these models, we tested Riluzole and E4031 applying dosages and routes of administrations already used and proven to be efficacious (Yip *et al*, 2009; Crociani *et al*, 2013; Speyer *et al*, 2016). We showed the capacity of the combination of the two drugs to improve Cisplatin antineoplastic effects. In particular (Figure 5C), we mimicked in mice the onset of chemoresistance in mice, treating the xenografted animals with full Cisplatin doses first and then with very low doses. In the latter case, tumours started to grow again, except when Riluzole and E4031 were included in the chemotherapeutic regimen. It is worth noting that the mouse model of chemoresistance we produced allowed us to unravel the effects of the combination, which was however masked by the intense effect of Cisplatin at full doses.

During CRC adjuvant therapy, the combination of Cisplatin (Oxaliplatin) with drugs that activate $K_{\text{Ca}3.1}$ and inhibit $K_{\text{v}11.1}$, such as Riluzole, may improve Cisplatin (Oxaliplatin) efficacy and overcome resistance in the clinical setting. Such combination would represent an example of personalised medicine in those patients who co-express $K_{\text{Ca}3.1}$ and $K_{\text{v}11.1}$ (Muratori *et al*, 2016). Importantly, Riluzole is already in clinical use for the treatment of

amyotrophic lateral sclerosis and is being investigated for the treatment of solid tumours in several clinical trials (<https://clinicaltrials.gov/>, NCT00903214 and NCT0086684). Of interest, Riluzole, showed preliminary benefit in a Phase 0 trial in patients with advanced melanoma and is currently in Phase 2 clinical trials (NCT0086684; Yip *et al*, 2009) and in Phase 1 for breast cancer (NCT00903214). Besides its effect on $K_{\text{Ca}3.1}$ and $K_{\text{v}11.1}$ in CRC cells, Riluzole may also enhance antitumour T-cell activity by overcoming the recently described ionic immune checkpoint (Eil *et al*, 2016). A combination of Riluzole with Cisplatin may show clinical benefit.

ACKNOWLEDGEMENTS

We thank Angelo Fortunato and Sara Falsini for helping in the first experiments with Cisplatin. This work was supported by Associazione Italiana per la Ricerca sul Cancro (AIRC, grant N°15627) to AA, by Associazione Noi per Voi Onlus to AA and ex 60% University of Firenze 2014 and 2015 to AA. TM thanks AIRC-FIRC (3-years' Fellowship for Italy, Project Code: 18044).

CONFLICT OF INTEREST

The authors declare no conflict of interest.

AUTHOR CONTRIBUTIONS

AA designed and supervised the whole study; SP, MD'A and GB performed cell viability, Annexin/PI assay and cell cycle analysis; GB and SP performed RQ-PCR analyses; LG and MD'A performed patch-clamp experiments; SP and GB performed Pt uptake experiments; TM, MS, RU and LM performed Pt uptake measurements; SP, GB and GP performed WB experiments; AG prepared silenced cells; SP, OC and GP performed *in vivo* experiments; AB revised patch-clamp data; KGC revised the paper and originally suggested the idea of evaluating Riluzole in colorectal tumours; AB and HW revised the paper; AA wrote the paper.

REFERENCES

- Arcangeli A, Crociani O, Lastraioli E, Masi A, Pillozzi S, Becchetti A (2009) Targeting ion channels in cancer: a novel frontier in antineoplastic therapy. *Curr Med Chem* **16**(1): 66–693.
- Barmeyer C, Rahner C, Yang Y, Sigworth FJ, Binder HJ, Rajendran VM (2010) Cloning and identification of tissue-specific expression of KCNN4 splice variants in rat colon. *Am J Physiol Cell Physiol* **299**(2): C251–C263.
- Barresi V, Trovato-Salinaro A, Spampinato G, Musso N, Castorina S, Rizzarelli E, Condorelli DF (2016) Transcriptome analysis of copper homeostasis genes reveals coordinated upregulation of SLC31A1, SCO1, and COX11 in colorectal cancer. *FEBS Open Bio* **6**(8): 794–806.
- Becchetti A, Arcangeli A, Del Bene MR, Olivetto M, Wanke E (1992) Intra and extracellular surface charges near Ca²⁺ channels in neurons and neuroblastoma cells. *Biophys J* **63**(4): 954–965.
- Carozzi VA, Canta A, Chiorazzi A (2015) Chemotherapy-induced peripheral neuropathy: What do we know about mechanisms? *Neurosci Lett* **596**: 90–107.
- Crociani O, Zanieri F, Pillozzi S, Lastraioli E, Stefanini M, Fiore A, Fortunato A, D'Amico M, Masselli M, De Lorenzo E, Gasparoli L, Chiu M, Bussolati O, Becchetti A, Arcangeli A (2013) hERG1 channels modulate integrin signaling to trigger angiogenesis and tumor progression in colorectal cancer. *Sci Rep* **3**: 3308.

- D'Amico M, Gasparoli L, Arcangeli A (2013) Potassium channels: novel emerging biomarkers and targets for therapy in cancer. *Recent Pat Anticancer Drug Discov* **8**(1): 53–65.
- Eil R, Vodnal SK, Clever D, Klebanoff CA, Sukumar M, Pan JH, Palmer DC, Gros A, Yamamoto TN, Patel SJ, Guittard GC, Yu Z, Carbonaro V, Okkenhaug K, Schrumpp DS, Linehan WM, Roychoudhuri R, Restifo NP (2016) Ionic immune suppression within the tumour microenvironment limits T cell effector function. *Nature* **537**(7621): 539–543.
- Galluzzi L, Vitale I, Michels J, Brenner C, Szabadkai G, Harel-Bellan A, Castedo M, Kroemer G (2014) Systems biology of Cisplatin resistance: past, present and future. *Cell Death Dis* **5**(5): e1257.
- Gasparoli L, D'Amico M, Masselli M, Pillozzi S, Caves R, Khuwaileh R, Tiedke W, Mugridge K, Pratesi A, Mitcheson JS, Basso G, Becchetti A, Arcangeli A (2015) New pyrimido-indole compound CD-160130 preferentially inhibits the KV11.1B isoform and produces antileukemic effects without cardiotoxicity. *Mol Pharmacol* **87**(2): 183–196.
- Huang CP, Fofana M, Chan J, Chang CJ, Howell SB (2014) Copper transporter 2 regulates intracellular copper and sensitivity to Cisplatin. *Metallomics* **6**(3): 654–661.
- Huang H, Zhu L, Reid BR, Drobny GP, Hopkins PB (1995) Solution structure of a cisplatin-induced DNA interstrand cross-link. *Science* **270**(5243): 1842–1845.
- Huang X, Jan LY (2014) Targeting potassium channels in cancer. *J Cell Biol* **206**(2): 151–162.
- Hui C, Lan Z, Yue-li L, Li-lin H, Li-lin H (2015) Knockdown of Eag1 expression by RNA interference increases chemosensitivity to Cisplatin in ovarian cancer cells. *Reprod Sci* **22**(12): 1618–1626.
- Ishida S, Lee J, Thiele DJ, Herskowitz I (2002) Uptake of the anticancer drug cisplatin mediated by the copper transporter Ctr1 in yeast and mammals. *Proc Natl Acad Sci USA* **99**(22): 14298–14302.
- Jentsch TJ, Lutter D, Planells-Cases R, Ullrich F, Voss FK (2016) RAC: molecular identification as LRR8 heteromers with differential functions. *Pflugers Arch* **468**(3): 385–393.
- Kalayda GV, Wagner CH, Buss I, Reedijk J, Jaehde U (2008) Altered localisation of the copper efflux transporters ATP7A and ATP7B associated with Cisplatin resistance in human ovarian carcinoma cells. *BMC Cancer* **8**: 175.
- Kartalou M, Essigmann JM (2001) Mechanisms of resistance to Cisplatin. *Mutat Res* **478**: 23–43.
- Katano K, Kondo A, Safaei R, Holzer A, Samimi G, Mishima M, Kuo YM, Rochdi M, Howell SB (2002) Acquisition of resistance to Cisplatin is accompanied by changes in the cellular pharmacology of copper. *Cancer Res* **62**(22): 6559–6565.
- Khan AJ, Wall B, Ahlawat S, Green C, Schiff D, Mehnert JM, Goydos JS, Chen S, Haffty BG (2011) Riluzole enhances ionizing radiation-induced cytotoxicity in human melanoma cells that ectopically express metabotropic glutamate receptor 1 in vitro and in vivo. *Clin Cancer Res* **17**(7): 1807–1814.
- Lang F, Hoffmann EK. Role of ion transport in control of apoptotic cell death (2012) *Compr Physiol* **2**(3): 2037–2061.
- Lastraioli E, Guasti L, Crociani O, Polvani S, Hofmann G, Witchel H, Bencini L, Calistri M, Messerini L, Scatizzi M, Moretti R, Wanke E, Olivotto M, Mugnai G, Arcangeli A (2004) herg1 gene and HERG1 protein are overexpressed in colorectal cancers and regulate cell invasion of tumor cells. *Cancer Res* **64**(2): 606–611.
- Lastraioli E, Perrone G, Sette A, Fiore A, Crociani O, Manoli S, D'Amico M, Masselli M, Iorio J, Callea M, Borzomati D, Nappo G, Bartolozzi F, Santini D, Bencini L, Farsi M, Boni L, Di Costanzo F, Schwab A, Onetti Muda A, Coppola R, Arcangeli A (2015) hERG1 channels drive tumour malignancy and may serve as prognostic factor in pancreatic ductal adenocarcinoma. *Br J Cancer* **112**(6): 1076–1087.
- Leanza L, O'Reilly P, Doyle A, Venturini E, Zoratti M, Szegezdi E, Szabo I (2014) Correlation between potassium channel expression and sensitivity to drug-induced cell death in tumor cell lines. *Curr Pharm Des* **20**(2): 189–200.
- Lee EL, Hasegawa Y, Shimizu T, Okada Y (2008) IK1 channel activity contributes to Cisplatin sensitivity of human epidermoid cancer cells. *Am J Physiol Cell Physiol* **294**(6): C1398–C1406.
- Marzo T, Pillozzi S, Hrabina O, Kasparkova J, Brabec V, Arcangeli A, Bartoli G, Severi M, Lunghi A, Totti F, Gabbiani C, Quiroga AG, Messori L (2015) cis-Pt I₂(NH₃)₂: a reappraisal. *Dalton Trans* **44**(33): 14896–14905.
- Matsumoto S, Tanaka T, Kurokawa H, Matsuno K, Hayashida Y, Takahashi T (2007) Effect of copper and role of the copper transporters ATP7A and CTR1 in intracellular accumulation of cisplatin. *Anticancer Res* **27**(4B): 2209–2216.
- Muratari L, Petroni G, Antonuzzo L, Boni L, Iorio J, Lastraioli E, Bartoli G, Messerini L, Di Costanzo F, Arcangeli A (2016) hERG1 positivity and Glut-1 negativity identifies high-risk TNM stage I and II colorectal cancer patients, regardless of adjuvant chemotherapy. *Onco Targets Ther* **9**: 6325–6332.
- Owatari S, Akune S, Komatsu M, Ikeda R, Firth SD, Che XF, Yamamoto M, Tsujikawa K, Kitazono M, Ishizawa T, Takeuchi T, Aikou T, Mercer JF, Akiyama S, Furukawa T (2007) Copper-transporting P-type ATPase, ATP7A, confers multidrug resistance and its expression is related to resistance to SN-38 in clinical colon cancer. *Cancer Res* **67**(10): 4860–4868.
- Pedersen SF, Klausen TK, Nilus B (2015) The identification of a volume-regulated anion channel: an amazing Odyssey. *Acta Physiol (Oxf)* **213**(4): 868–881.
- Pillozzi S, Brizzi MF, Bernabei PA, Bartolozzi B, Caporale R, Basile V, Boddi V, Pegoraro L, Becchetti A, Arcangeli A (2007) VEGFR-1 (FLT-1), beta1 integrin, and hERG K⁺ channel for a macromolecular signaling complex in acute myeloid leukemia: role in cell migration and clinical outcome. *Blood* **110**(4): 1238–1250.
- Pillozzi S, Masselli M, De Lorenzo E, Accordi B, Cilia E, Crociani O, Amedei A, Veltroni M, D'Amico M, Basso G, Becchetti A, Campana D, Arcangeli A (2011) Chemotherapy resistance in acute lymphoblastic leukemia requires hERG1 channels and is overcome by hERG1 blockers. *Blood* **117**(3): 902–914.
- Pillozzi S, Masselli M, Gasparoli L, D'Amico M, Polletta L, Veltroni M, Favre C, Basso G, Becchetti A, Arcangeli A (2016) Macrolide antibiotics exert antileukemic effects by modulating the autophagic flux through inhibition of hERG1 potassium channels. *Blood Cancer J* **6**: e423.
- Planells-Cases R, Lutter D, Guyader C, Gerhards NM, Ullrich F, Elger DA, Kucukosmanoglu A, Xu G, Voss FK, Reincke SM, Stauber T, Blomen VA, Vis DJ, Wessels LF, Brummelkamp TR, Borst P, Rottenberg S, Jentsch TJ (2015) Subunit composition of VRAC channels determines substrate specificity and cellular resistance to Pt-based anti-cancer drugs. *EMBO J* **34**(24): 2993–3008.
- Poulsen KA, Andersen EC, Hansen CF, Klausen TK, Hougaard C, Lambert IH, Hoffmann EK (2010) Deregulation of apoptotic volume decrease and ionic movements in multidrug-resistant tumor cells: role of chloride channels. *Am J Physiol Cell Physiol* **298**(1): C14–C25.
- Samuel P, Pink RC, Caley DP, Currie JM, Brooks SA, Carter DR (2016) Over-expression of miR-31 or loss of KCNMA1 leads to increased cisplatin resistance in ovarian cancer cells. *Tumour Biol* **37**(2): 2565–2573.
- Sanguinetti MC, Jurkiewicz NK (1990) Two components of cardiac delayed rectifier K⁺ current: differential sensitivity to block by class III antiarrhythmic agents. *J Gen Physiol* **96**: 195–215.
- Sankaranarayanan A, Raman G, Busch C, Schultz T, Zimin PI, Hoyer J, Köhler R, Wulff H (2009) Naphtho[1,2-d]thiazol-2-ylamine (SKA-31), a new activator of KCa2 and KCa3.1 potassium channels, potentiates the endothelium-derived hyperpolarizing factor response and lowers blood pressure. *Mol Pharmacol* **75**(2): 281–295.
- Shimizu T, Lee EL, Ise T, Okada Y (2008) Volume-sensitive Cl⁻ channel as a regulator of acquired Cisplatin resistance. *Anticancer Res* **28**(1A): 75–83.
- Siddik ZH (2003) Cisplatin: mode of cytotoxic action and molecular basis of resistance. *Oncogene* **22**: 7265–7279.
- Speyer CL, Nassar MA, Hachem AH, Bukhsh MA, Jafry WS, Khansa RM, Gorski DH (2016) Riluzole mediates anti-tumor properties in breast cancer cells independent of metabotropic glutamate receptor-1. *Breast Cancer Res Treat* **157**(2): 217–228.
- Spitzner M, Ousingsawat J, Scheidt K, Kunzelmann K, Schreiber R (2007) Voltage-gated K⁺ channels support proliferation of colonic carcinoma cells. *FASEB J* **21**(1): 35–44.
- Stefani A, Spadoni F, Bernardi G (1997) Differential inhibition by riluzole, lamotrigine, and phenytoin of sodium and calcium currents in cortical neurons: implications for neuroprotective strategies. *Exp Neurol* **147**(1): 115–122.
- Syeda R, Qiu Z, Dubin AE, Murthy SE, Florendo MN, Mason DE, Mathur J, Cahalan SM, Peters EC, Montal M, Patapoutian A (2016) LRR8 proteins form volume-regulated anion channels that sense ionic strength. *Cell* **164**: 499–511.
- Wang D, Lippard SJ (2005) Cellular processing of platinum anticancer drugs. *Nat Rev Drug Discov* **4**: 307–320.

- Wang YJ, Lin MW, Lin AA, Wu SN (2008) Riluzole-induced block of voltage-gated Na⁺ current and activation of BKCa channels in cultured differentiated human skeletal muscle cells. *Life Sci* **82**(1-2): 11–20.
- Wong RS (2011) Apoptosis in cancer: from pathogenesis to treatment. *J Exp Clin Cancer Res* **30**(1): 87–101.
- Wulff H, Miller MJ, Hansel W, Grissmer S, Cahalan MD, Chandy KG (2000) Design of a potent and selective inhibitor of the intermediate-conductance Ca²⁺-activated K⁺ channel, IKCa1: a potential immunosuppressant. *Proc Natl Acad Sci USA* **97**(14): 8151–8156.
- Yip D, Le MN, Chan JL, Lee JH, Mehnert JA, Yudd A, Kempf J, Shih WJ, Chen S, Goydos JS (2009) A phase 0 trial of riluzole in patients with resectable stage III and IV melanoma. *Clin Cancer Res* **15**(11): 3896–3902.
- Yoshida M, Khokhar AR, Siddik ZH (1994) Biochemical pharmacology of homologous alicyclic mixed amine platinum(II) complexes in sensitive and resistant tumor cell lines. *Cancer Res* **54**: 3468–3473.
- Zhang R, Tian P, Chi Q, Wang J, Wang Y, Sun L, Liu Y, Tian S, Zhang Q (2012) Human ether-à-go-go-related gene expression is essential for Cisplatin to induce apoptosis in human gastric cancer. *Oncol Rep* **27**(2): 433–440.

This work is published under the standard license to publish agreement. After 12 months the work will become freely available and the license terms will switch to a Creative Commons Attribution-NonCommercial-Share Alike 4.0 Unported License.

Supplementary Information accompanies this paper on British Journal of Cancer website (<http://www.nature.com/bjc>)